Low Profile Intelligent Reflecting Metasurface for B5G Applications

Monisha Selvaraj
SASTRA Deemed to be University
Ramya Vijay (ramyavijay@ieee.org)
SASTRA Deemed to be University
Rajesh Anbazhagan
SASTRA Deemed to be University

Research Article

Keywords: B5G, Frequency Selective Metasurface, Intelligent Reflecting Surface, Polarization Insensitivity

Posted Date: April 11th, 2022

DOI: https://doi.org/10.21203/rs.3.rs-1528047/v1

Abstract

In this letter, an intelligent reflecting single-layer frequency selective metasurface is presented for beyond fifth-generation (B5G) applications. The proposed unit cell comprises of a novel complementary loop to achieve wider impedance bandwidth of 0.70 – 0.96 THz with high angular stability and better polarization insensitivity. The modified complementary loop structure is etched on a gold-layered polydimethylsiloxane substrate that displays a stable resonance frequency for possible incident angles. The reflecting unit cell with negative permeability has a peak reflection coefficient of -24.19 dB at 0.82 THz. Here, an equivalent circuit model is used to analyse a proposed FSS in the THz range.

1. Introduction

The deployment of the Fifth-Generation (5G) wireless communication is realized in various countries and counting. Presently, the research community and industry are looking forward for beyond 5G (B5G) communications due to high demands on coverage, ultra-high data rates, energy efficiency, and reliability [1]. In the literature, technologies viz., cognitive radio (CR) [2], cooperative communications [3], and multiple-input multiple-output (MIMO) [4] are explored to meet the requirements of 5G networks. Though these technologies improve bandwidth and energy efficiency with intelligent signal processing at the transceiver, limited research is being carried out to address the uncontrollable electromagnetic (EM) wave propagation [5].

In recent times, intelligent reflecting surface (IRS) is a potential approach to achieve wider bandwidth and efficiency for controlling the wireless environment. IRS modifies the scattering and attenuation of an incident wave before it reaches the target receiver with the help of a pre-programmed controller, a smartly manageable wireless system. However, the futuristic wireless scenario motivates us to optimize the EM wave propagation using IRS for B5G systems [6]. IRS architecture includes a controller, a massive number of periodic metallic reconfigurable elements, and conducting plates. The IRS controller serves as a gateway and allows the network components to communicate to the end devices [7]. Moreover, frequency selective surface (FSS) can act as a periodic metallic structure that changes the electromagnetic architecture of buildings (EAoB) to manage security and spectral efficiency.

Conventional FSS are narrowband and do not offer effective spatial filtering responses [8]. Besides, wideband FSS with improved frequency response, angular stability, and dual-polarization is a key research area [9]. Based on Munk's concept [10], FSS elements with closed-loop structures display excellent angular stability. However, the better angular stability with polarization-insensitive encourages further research. In this letter, a novel compact single-layer reflecting metasurface with better angular stability and polarization-insensitivity. Till now, FSS at THz has been primarily used as an absorber. Here, the novelty of this work is to design THz FSS as low profile intelligent reflecting metasurface for IRS applications.

2. Design Methodology And Equivalent Circuit Model

Figure 1 illustrates the structure of proposed THz reflecting metasurface imposed on a gold layered polydimethylsiloxane dielectric material ($\varepsilon_r = 2.35$) with the unit cell dimension of 100×100×10 um^3. The reflecting structure is designed with three phases to attain the desired characteristics.

In the first phase, a conventional slotted square loop element is constructed as shown in Fig. 2(a) for 0.82 THz. The initial design is simulated with the finite element method, and its essential characteristics are analysed using an equivalent circuit model [11] as displayed in Fig. 2(b).

The equivalent circuit model for slotted square loop is developed using (1)-(7) [12],

$$L_1 = \frac{X_{L11}}{Z_0} = \cos\theta F(p, g, , \theta)$$

1

$$k = p - 2s, l = d - 2s$$

2

$$U = \frac{X_{L21}}{Z_0} = \frac{k}{p}\cos\theta F(p, l, , \theta)$$

3

$$L_2 = \frac{X_{L22}}{Z_0} = U + \frac{s}{l+g}L_1$$

4

$$L = \frac{C_1}{Y_0} = 4\sec\theta F(p, d, , \theta)$$

5

$$M = \frac{C_2}{Y_0} = 4\sec\theta F(d - s, s, , \theta)$$

6

$$C_1 = \frac{C}{Y_0} = (1.75L + 0.6M)_{eff}$$

7

In (1), L1 denotes the inductance of the outer square loop with g width. L2 in (4) denotes the inductance of inward squares (with l sides) influenced by L1. The capacitance value from (7) is attained from

equations (5) and (6).

To improve the bandwidth and angular stability compared with the conventional design, four slits on the corner of the inner square are introduced as presented in Fig. 3(a) and the corresponding equivalent circuit model is shown in Fig. 3(b).

In third phase, a three-legged slit is introduced to increase the angular stability and polarization insensitivity as shown in Fig. 4(a). Further, Fig. 4(b) depicts its equivalent circuit model. Table 1 presents the structural parameter values of the proposed design.

TABLE I Dimensions of the Proposed Unit Cell

Parameter	d	p	S	g	L	W	G
Dimension (um)	85	100	15	15	19.42	2	5

3. Results And Discussions

3.1. Configuration Analysis

Figure 5(a) illustrates the reflection coefficients of the various configurations. The proposed unit cell has a broader impedance bandwidth of 23.08% than the conventional slotted square loop with better angular stability and polarization insensitivity at various oblique incident angles. Further, the reflecting unit cell was compared and analysed with an equivalent circuit model. Figure 5(b) displays good agreement between the proposed structure and the mathematical model.

3.2. Parametric Analysis

The distribution of the generated current can be controlled by choosing appropriate cell structure parameters, which results in desired transmission properties. The operating frequency of the FSS is affected by the unit structure characteristics and the operational bandwidth, insertion loss, oblique incidence stability, and polarisation stability. As a result, the effect of changing the width of the slotted square loop and G value on the frequency response characteristics of the proposed FSS has been investigated.

Figure 6(a-b) illustrates the bandwidth enhancement for different square slot width dimensions and G. The loop perimeter is chosen nearly equal to the resonating wavelength. The study discloses the relation between the loop width and impedance bandwidth.

3.3. Angular Stability

The choice of FSS structure is sensitive to the incident angle and displays a substantial variance at its resonance frequency due to the uncertainty of the direction of the EM wave. At high variance, the FSS

does not maintain the spatial filtering characteristics. The angular stability under various incidence angles for TE & TM modes of operations can be calculated using the angle mean deviation (AMD) [13].

Figure 7 represents the comparison of AMD for various configurations at different angles. The AMD of the operating frequency is reduced up to 2.99% at TE mode and 0.53% at TM mode. It is evident that the variation in AMD percentage for the proposed reflective unit cell demonstrate an angular stability of 97.01% at TE modes and 99.47% at TM mode.

3.4. Polarization Insensitivity

In FSS, the influence of the incident angle of the EM wave and polarization mode is non–measurable. The FSS structure must have a stable frequency at both TE and TM polarized incident waves to have polarization insensitivity.

Figure 8 shows the reflecting coefficient for the proposed FSS unit cell with various polarization under normal incidence angle (consider θ = 60°, due to angular stability). The designed unit cell has a stable resonating frequency at different angles. The average maximum deviation rate of the resonating frequency of the proposed unit cell with various polarized angles is approximately 0.27%, proving the better polarization insensitivity.

3.5. Metasurface Analyses

The amplitude of effective permeability and permittivity are shown in Fig. 9a and Fig. 9b, respectively. The effective medium exhibits the negative peaks in frequency response of 0.82 GHz. In Fig. 9b, the permeability curve gives the negative real values from 0.7 THz. The intelligent reflecting metasurface exhibits the negative permeability and permittivity at 0.82 THz, ensuring the proposed meta-surface satisfies the left-handed characteristic.

Further, a comparative study was carried out and reported in Table II to demonstrate the uniqueness of the projected FSS over the previous designs [14–16]. The operating band, number of layers, bandwidth, polarisation insensitivity, and degree of angular stability are compared. Though [15] provides greater bandwidth, the proposed intelligent reflecting meta surface accomplishes better angular stability and polarization insensitivity with an adequate bandwidth.

TABLE II Comparison of the Proposed Unit Cell with other related FSS Structure

Ref.	Operating Frequency (In THz)	Layer	Impedance Bandwidth (In THz)	Polarization insensitivity	Angular stability
[14]	2.11	Single-sided single layer	0.013	No	70°
[15]	0.775	Multilayer	1.450	No	60°
[16]	0.5	Multilayer	-	Yes	60°
This work	0.82	Single-sided single layer	0.260	Yes	180°

4. Conclusion

A low profile slotted meta-atom was designed to obtain angular stability, polarization-insensitive and wideband reflecting metasurface. It displays a reflection band of 0.82 THz, which covers a bandwidth of 260 GHz. the results prove that the unit cell is suitable for normal and oblique angles of incidence wave. The intelligent reflecting metasurface finds its application to reduce the information loss during non-line sight.

Declarations

Funding

- The authors did not receive support from any organization for the submitted work.
- No funding was received to assist with the preparation of this manuscript.
- No funding was received for conducting this study.
- No funds, grants, or other support was received.

Conflict of interest / Competing interests

The Authors confirm that there are no known conflicts of interest associated with this publication and there has been no significant financial support for this work that could have influenced its outcome.

Availability of data and material

The authors declare that any data related to this research will be made available on request.

Code availability

The authors declare that any code related to this research will be made available on request.

Authors' Contribution

All Authors are responsible for the correctness of the statements provided in the manuscript. The following contributions have been made by the Authors. The design of Reflecting Metasurface and analysis has been made by Author 1. Author 2 has made interpretation and the conceptual idea of reflecting surface. The Metasurface analysis has been made by Author 3.

Ethics approval

The Authors declare that this research does not contain any studies with animal or human subjects.

Consent to participate

The authors declare that that this research does not contain any studies with humans or individual participants.

Consent for publication

The authors declare that that this research does not contain any studies with individuals or patients and hence no data is associated to be published.

References

1. Ebrahimi, A., Ako, R.T., Lee, W.S.L., Bhaskaran, M., Sriram, S., Withayachumnankul, W.: High-Q Terahertz Absorber with Stable Angular Response. IEEE Trans. Terahertz Sci. Technol. 10, 204–211 (2020). https://doi.org/10.1109/TTHZ.2020.2964812
2. Mohammadi Nemat-Abad, H., Zareian-Jahromi, E., Basiri, R.: Design and equivalent circuit model extraction of a third-order band-pass frequency selective surface filter for terahertz applications. Eng. Sci. Technol. an Int. J. 22, 862–868 (2019). https://doi.org/10.1016/J.JESTCH.2019.01.008
3. Patel, S.K., Sorathiya, V., Lavadiya, S., Nguyen, T.K., Dhasarathan, V., Patel, S.K., Sorathiya, V., Lavadiya, S., Nguyen, T.K., Dhasarathan, V.: Polarization insensitive graphene-based tunable frequency selective surface for far-infrared frequency spectrum. PhyE. 120, 114049 (2020). https://doi.org/10.1016/J.PHYSE.2020.114049
4. Paul, G.S., Mandal, K.: Polarization-insensitive and angularly stable compact ultrawide stop-band frequency selective surface. IEEE Antennas Wirel. Propag. Lett. 18, 1917–1921 (2019). https://doi.org/10.1109/LAWP.2019.2933545
5. Ferreira, D., Caldeirinha, R.F.S., Cuinas, I., Fernandes, T.R.: Square Loop and Slot Frequency Selective Surfaces Study for Equivalent Circuit Model Optimization. IEEE Trans. Antennas Propag. 63, 3947–3955 (2015). https://doi.org/10.1109/TAP.2015.2444420
6. Govindanarayanan, I., Rangaswamy, N., Anbazhagan, R.: Design and analysis of broadband magneto-electric dipole antenna for LTE femtocell base stations. J. Comput. Electron. 15, 200–209 (2016). https://doi.org/10.1007/S10825-015-0759-0/TABLES/3
7. Munk, B. (Benedikt A..: Frequency selective surfaces: theory and design. John Wiley (2000)

8. Bouslama, M., Traii, M., Denidni, T.A., Gharsallah, A.: Reconfigurable frequency selective surface for beam-switching applications. IET Microwaves, Antennas Propag. 11, 69–74 (2017). https://doi.org/10.1049/IET-MAP.2016.0080/CITE/REFWORKS
9. Monisha, S., Ramya Vijay,: 2-Dimensional Reconfigurable Reflecting Unit Cell for THz Communication. 2021 IEEE International Conference on Advanced Networks and Telecommunications Systems (ANTS),
10. Chen, J., Liang, Y.C., Pei, Y., Guo, H.: Intelligent Reflecting Surface: A Programmable Wireless Environment for Physical Layer Security. IEEE Access. 7, 82599–82612 (2019). https://doi.org/10.1109/ACCESS.2019.2924034
11. Wu, Q., Zhang, S., Zheng, B., You, C., Zhang, R.: Intelligent Reflecting Surface Aided Wireless Communications: A Tutorial. IEEE Trans. Commun. 69, 3313–3351 (2020). https://doi.org/10.48550/arxiv.2007.02759
12. Liaskos, C., Nie, S., Tsioliaridou, A., Pitsillides, A., Ioannidis, S., Akyildiz, I.: A New Wireless Communication Paradigm through Software-Controlled Metasurfaces. IEEE Commun. Mag. 56, 162–169 (2018). https://doi.org/10.1109/MCOM.2018.1700659
13. Liang, Y.C., Chen, K.C., Li, G.Y., Mähönen, P.: Cognitive radio networking and communications: An overview. IEEE Trans. Veh. Technol. 60, 3386–3407 (2011). https://doi.org/10.1109/TVT.2011.2158673
14. Nosratinia, A., Hunter, T.E., Hedayat, A.: Cooperative communication in wireless networks. IEEE Commun. Mag. 42, 74–80 (2004). https://doi.org/10.1109/MCOM.2004.1341264
15. Rusek, F., Persson, D., Lau, B.K., Larsson, E.G., Marzetta, T.L., Edfors, O., Tufvesson, F.: Scaling up MIMO: Opportunities and challenges with very large arrays. IEEE Signal Process. Mag. 30, 40–60 (2013). https://doi.org/10.1109/MSP.2011.2178495
16. Rajatheva, N., Atzeni, I., Bicais, S., Bjornson, E., Bourdoux, A., Buzzi, S., D'Andrea, C., Dore, J.-B., Erkucuk, S., Fuentes, M., Guan, K., Hu, Y., Huang, X., Hulkkonen, J., Jornet, J.M., Katz, M., Makki, B., Nilsson, R., Panayirci, E., Rabie, K., Rajapaksha, N., Salehi, M., Sarieddeen, H., Shahabuddin, S., Svensson, T., Tervo, O., Tolli, A., Wu, Q., Xu, W.: Scoring the Terabit/s Goal:Broadband Connectivity in 6G. (2020). https://doi.org/10.48550/arxiv.2008.07220

Figures

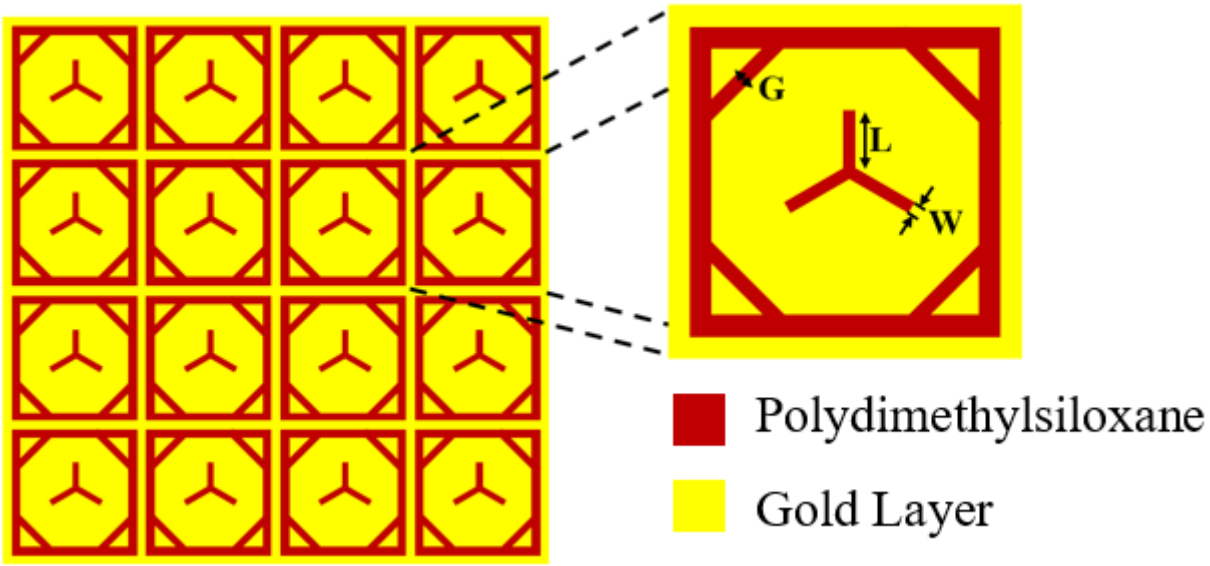

Figure 1

Proposed THz Intelligent Reflecting Surface

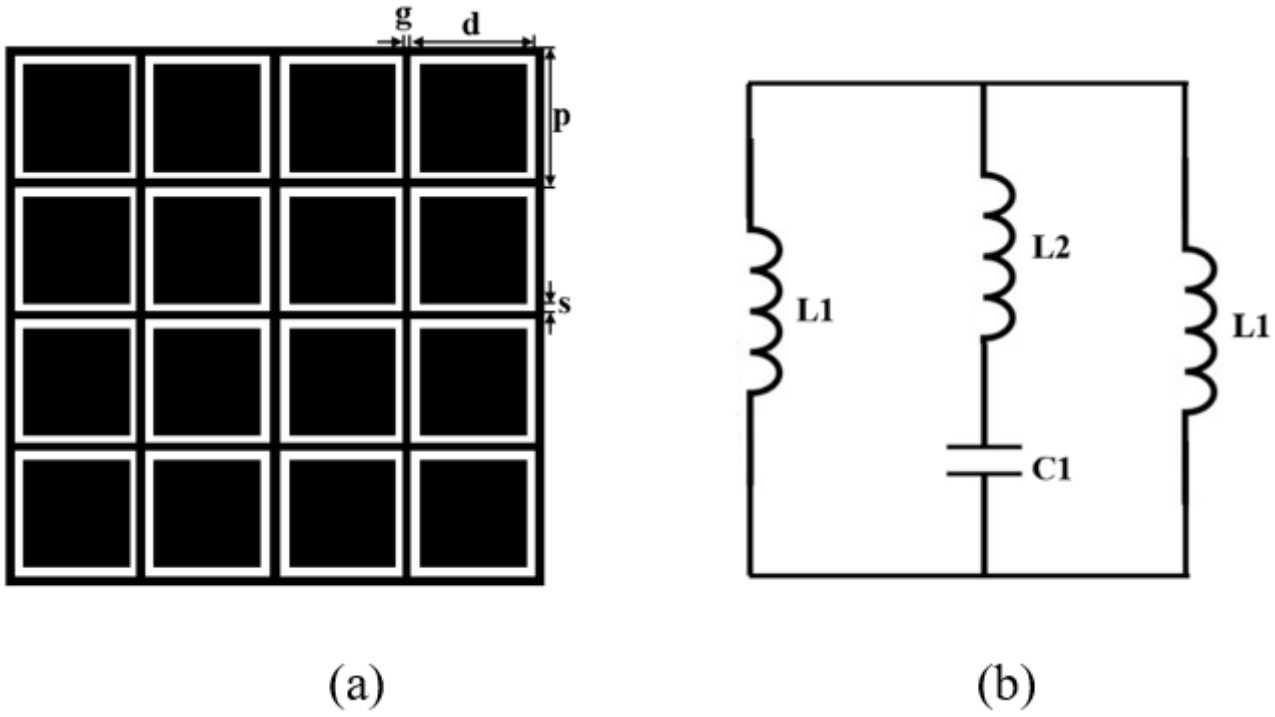

Figure 2

(a) 1st Configuration (Conventional slotted square loop) (b) Corresponding Equivalent Circuit Model

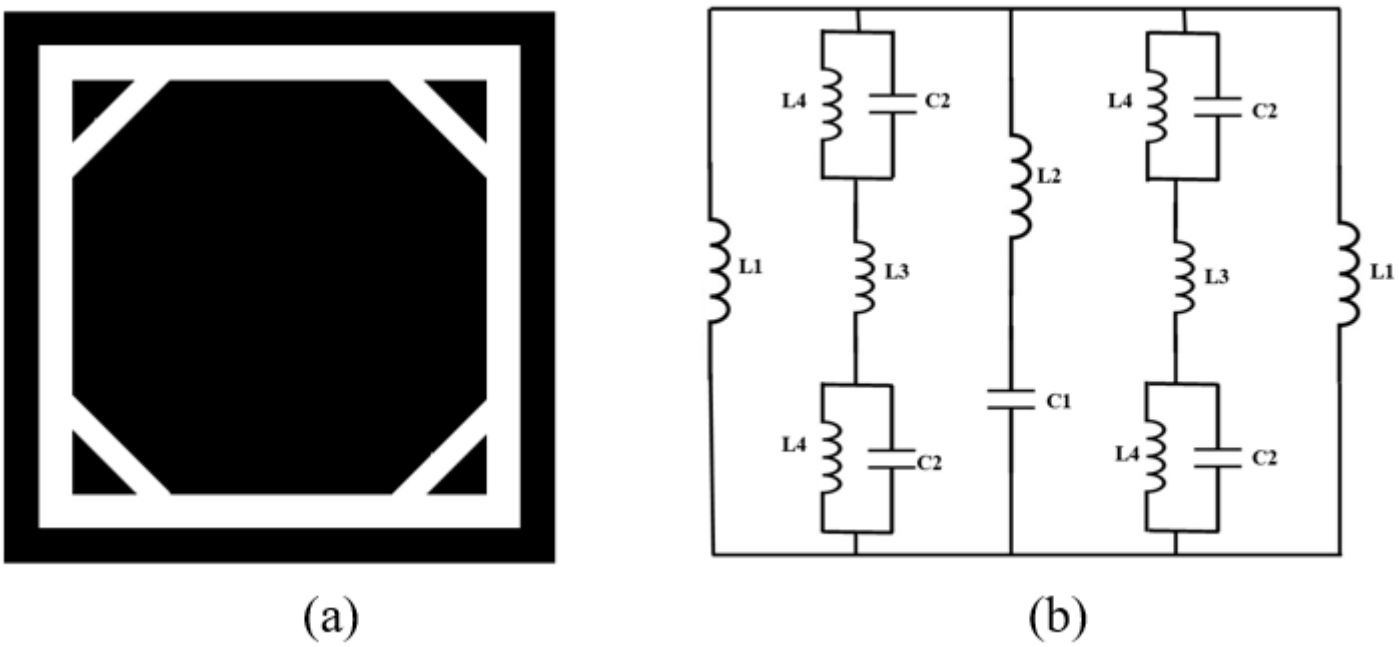

Figure 3

(a) 2nd Configuration (Slits on four corners) (b) Corresponding Equivalent Circuit Model

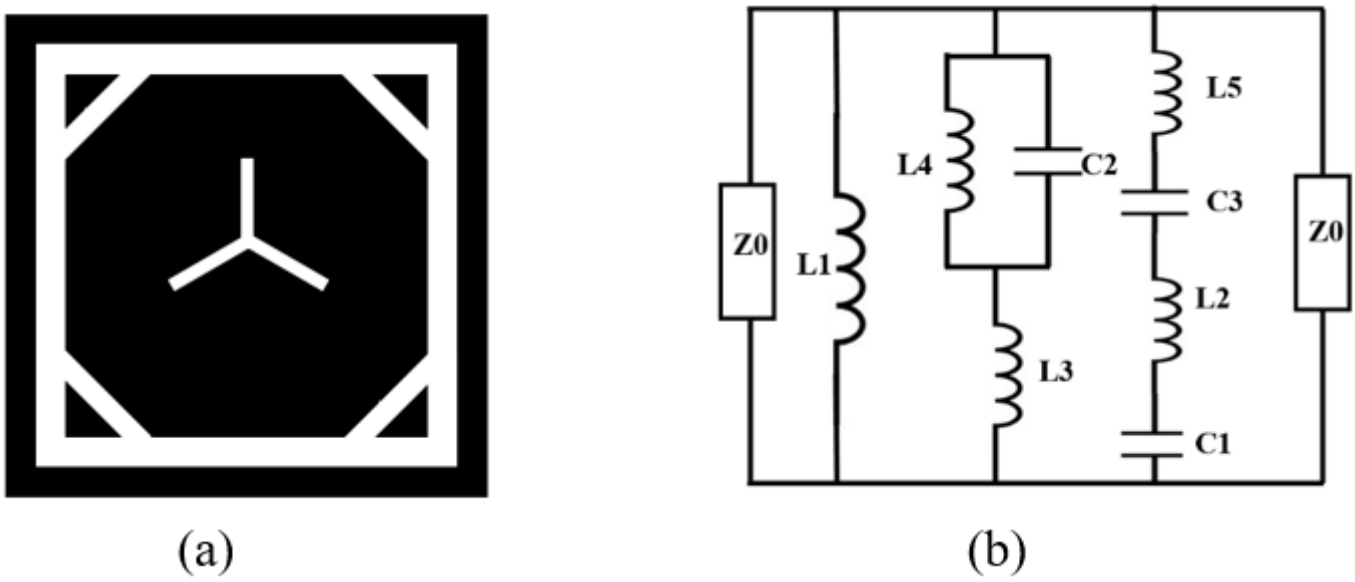

Figure 4

(a) 3rd Configuration (slotted three-legged element) (b) Corresponding modified Equivalent Circuit Model

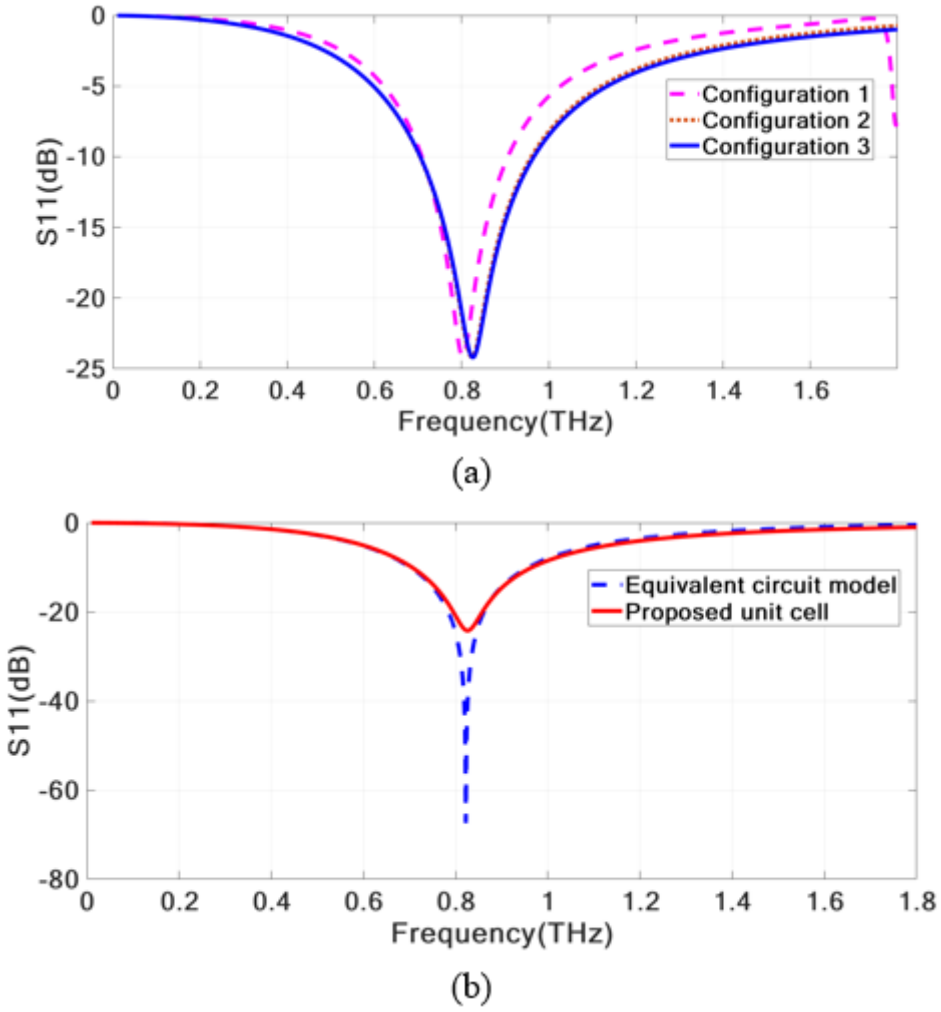

Figure 5

(a) Configurations of the proposed unit cell (b) Comparison with the equivalent circuit

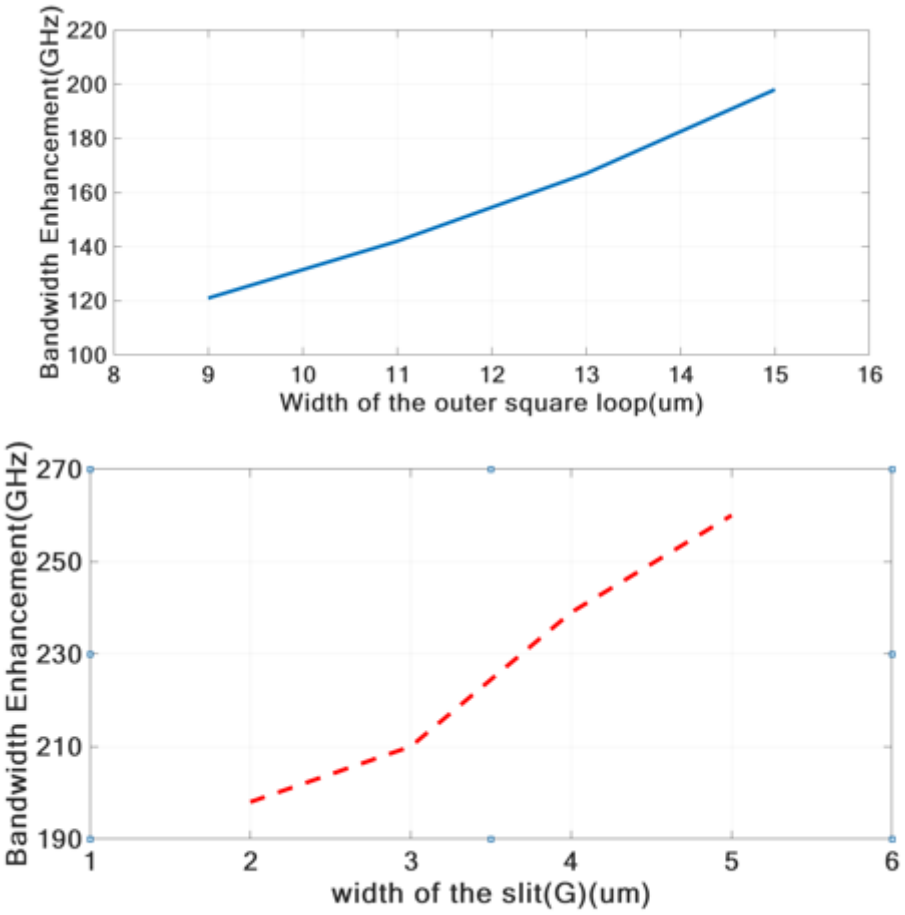

Figure 6

(a) Bandwidth Enhancement vs Slot width (b) Bandwidth Enhancement vs G

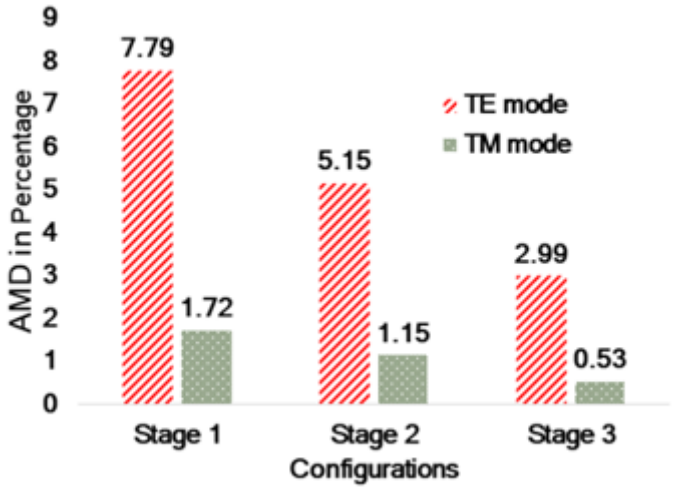

Figure 7

Graph for AMD% for different configurations

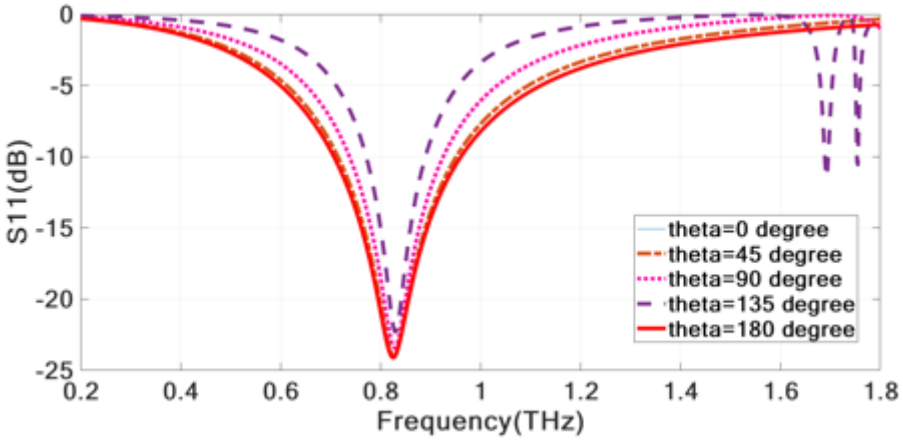

Figure 8

Reflection coefficient for various polarization angles at q=60°

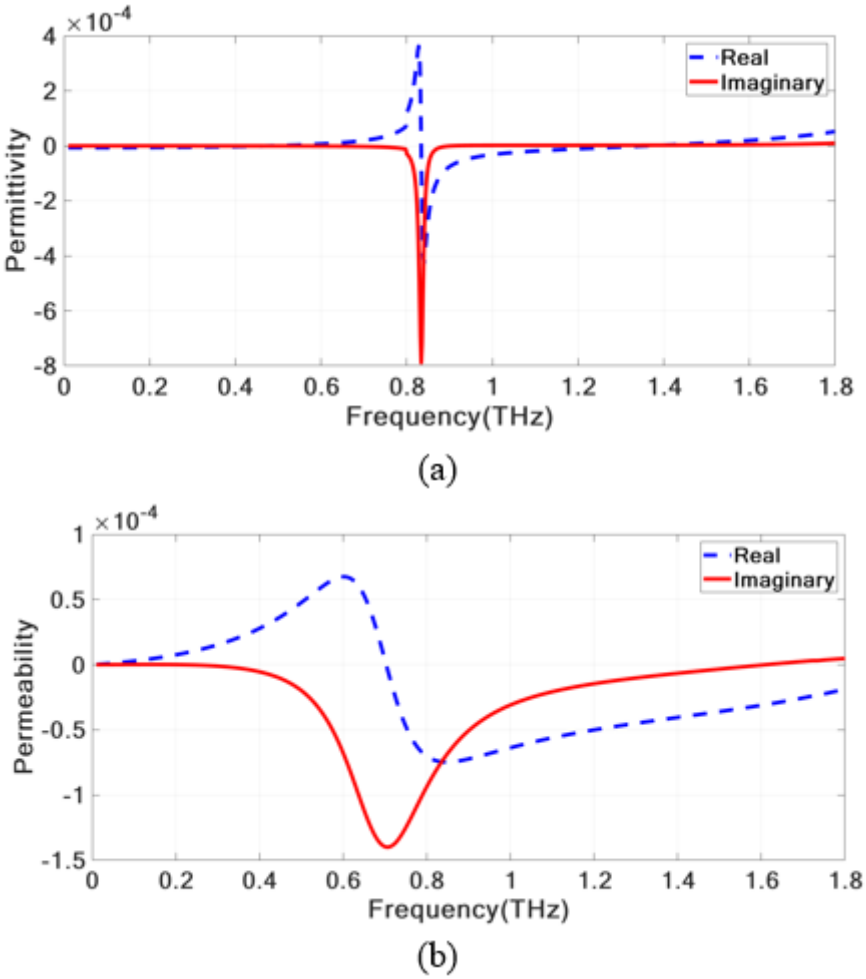

Figure 9

(a) Effective permittivity (b) Effective Permeability